Synergistic Interaction between Substrate and Seed Particles in Ultrathin Ultrananocrystalline Diamond Film Nucleation on SiO 2 with Controlled Surface Termination

ARTICLE *in* THE JOURNAL OF PHYSICAL CHEMISTRY C · APRIL 2012

Impact Factor: 4.77 · DOI: 10.1021/jp2117328

3 AUTHORS:

Hak-Joo Lee
Korea Institute of Science and Technology
18 PUBLICATIONS **55** CITATIONS
SEE PROFILE

Hyeongtag Jeon
Hanyang University
208 PUBLICATIONS **1,848** CITATIONS
SEE PROFILE

Wook-Seong Lee
Korea Institute of Science and Technology
55 PUBLICATIONS **224** CITATIONS
SEE PROFILE

THE JOURNAL OF PHYSICAL CHEMISTRY C

Article

pubs.acs.org/JPCC

Synergistic Interaction between Substrate and Seed Particles in Ultrathin Ultrananocrystalline Diamond Film Nucleation on SiO_2 with Controlled Surface Termination

Hak-Joo Lee,[†,‡] Hyeongtag Jeon,[‡] and Wook-Seong Lee*[,†]

[†]Electronic Materials Center, Korea Institute of Science and Technology, Hwarang-ro 14-gil, Seongbuk-gu, Seoul 136-791, Republic of Korea

[‡]Department of Materials Science and Engineering, Hanyang University, Wangsimni-ro 222, Seongdong-gu, Seoul 133-791, Republic of Korea

ABSTRACT: We have investigated the effect of surface modification on the dispersion of nanodiamond seeds on the SiO_2-coated Si substrate, to enable the ultrathin ultrananocrystalline diamond (UNCD) coating on the substrate, by direct current plasma-assisted chemical vapor deposition (DC-PACVD) using hydrogen-rich chemistry. The ultrasonically dispersed seed density on the SiO_2-coated Si wafer was so much lower than that on the pristine Si wafer that the void-free ultrathin UNCD coating was impossible. For surface modification, we have exposed the substrate to (1) the hydrogen/hydrocarbon plasma in the DC-PACVD chamber or (2) the hydrocarbon atmosphere in the hot filament chemical vapor deposition (HF-CVD) chamber, prior to the ultrasonic seeding. The exposure to hydrocarbon or to its plasma greatly reduced the seed density, while exposure to hydrogen plasma drastically enhanced it by a factor of 6, which enabled a void-free ultrathin UNCD coating as thin as 30 nm. The UNCD film and the substrate surface before and after the surface treatment were characterized by XPS, NEXAFS, FTIR, Raman spectroscopy, HR-SEM, HR-TEM, EDX, and the zeta potential analyzer. The effects of the pretreatments on the seed density were explained by Si−OH or Si−CH_3 termination and by the consequent change on (1) the zeta potentials of the substrate and (2) that of the nanodiamond particles in the seeding suspension.

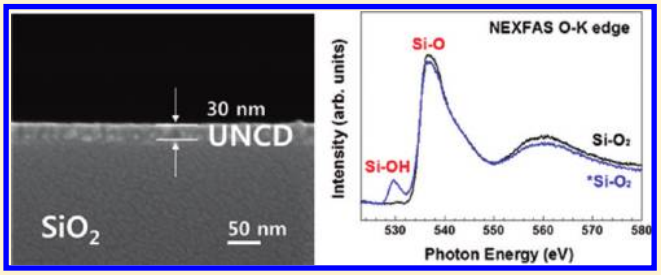

1. INTRODUCTION

The nanocrystalline or ultrananocrystalline diamond (NCD and UNCD, respectively) thin film has opened an innovative route for a wide variety of applications.[1−6] In particular, the ultrathin (less than 100 nm in thickness) diamond coating on the SiO_2-coated Si wafer is important for nanoelectromechanical system (NEMS) applications,[7,8] which utilize the ultrathin diamond layer.[5,8−10] Other important examples of the ultrathin diamond layer are (1) a hermetic coating over the delicate 3-dimentional geometry of the microelectrode arrays for implanted retinal prosthesis,[11−13] where the thin conformal UNCD layer was proved to be one of the best choices and (2) a localized surface plasmon resonance (LSPR) sensor using the thin diamond layer as the dielectric layer, where the diamond layer should be as thin as possible to enable a sensitive plasmonics sensing.[14]

Nevertheless, it is not easy to synthesize the ultrathin void-free diamond layer on the SiO_2 surface, due to the low nucleation density[15,16] and long incubation time compared to that on the pristine Si substrate.[17] It is particularly true when the hydrogen-rich, rather than the Ar-rich, precursor gas chemistry is adopted for the synthesis since the high concentration of atomic hydrogen in the former gas chemistry results in the reduction of the nucleation rate due to its etching action.[1,3,5] Nevertheless, the use of the hydrogen-rich precursor gas is still prevailing for NCD/UNCD synthesis,[5] probably due to a better plasma stability in microwave plasma chemical vapor deposition (MW-CVD) or direct current plasma-assisted chemical vapor deposition (DC-PACVD) or due to a much wider gas composition window in hot filament chemical vapor deposition (HF-CVD), where the filament contamination by solid carbon is prevented.

The bias enhanced nucleation (BEN) technique has been widely adopted for enhancing nucleation for diamond coating on the Si wafer.[18−21] However, since it is limited to the conducting substrate,[22] its application to the SiO_2-coated Si wafer is problematic, due to the low conductivity at the usual UNCD deposition temperature.[23,24]

Ultrasonic treatment of the substrate immersed in the diamond powder suspension was also widely adopted for nucleation enhancement.[25−27] For the *microcrystalline* diamond film deposition, where the *microcrystalline* diamond particle suspension was used for ultrasonic substrate treatment, it was initially argued that the nucleation was enhanced by the scratching of the substrate surface by the diamond particle.[25] It

Received: December 6, 2011
Revised: March 28, 2012
Published: April 9, 2012

   dx.doi.org/10.1021/jp2117328 | *J. Phys. Chem. C* 2012, 116, 9180−9188

Table 1. Experimental Conditions for the Substrate Treatment and UNCD Deposition

process	experimental parameters							
	gas composition	total gas flow [sccm]	pressure [Torr]	time [min]	CVD system	discharge/filament voltage [V]	discharge/filament current [A]	substrate temperature [°C]
(*)hydrogen plasma treatment	100% H_2	150	30	5	DC-PACVD	450	25	below 500
(†)hydrocarbon plasma treatment	6% CH_4 94% H_2	150	30	30	DC-PACVD	450	25	below 500
(‡)hydrocarbon thermal treatment	6% CH_4 94% H_2	150	30	30	HF-CVD	50	220	800
ultrasonic treatment	Ultrasonic Seeding: using nanodiamond mixed methanol for 60 min Ultrasonic Cleaning: using ethanol for 30 s (3 times)							
UNCD deposition	3% CH_4 97% H_2	150	80	10−240	DC-PACVD	450	25	750−800

was subsequently discovered that the diamond debris remaining on the surface was responsible.[26]

By contrast, for ultrasonic substrate treatment for the *nanocrystalline* diamond deposition, *nanodiamond* suspension was used. It was only recently that the transfer of nanodiamond particles from the suspension to the substrate was suggested as a seeding mechanism.[27−30] In this context, various efforts were made to enhance the dispersion of the transferred particles on the substrate: functionalization of the seed diamond particle surface[28,30−32] and addition of surfactant to,[33−35] or controlling the pH of, the suspension.[35−37] Furthermore, ball-milling of the diamond powder using ceramic bead[27,35,38] or annealing in contact with hydrogen[39] were also adopted to remove/break the strong sp^2 carbon bond between individual nanodiamond particles for monodispersion of the seeds.

However, such efforts were directed exclusively to the seed *diamond particles* in the suspension, not to *the substrate* onto which the seed is transferred. By contrast, it is reasonable to expect an electrostatic charging of the substrate surface during the ultrasonic treatment. It follows that the transfer of the nanodiamond particle from the suspension to the substrate will be driven by the electrostatic interaction between the particles and the substrate, in addition to that between the particles. Thus, enabling the control over the electrostatic nature of the substrate, in addition to that of the nanodiamond particle, will significantly expand the parameter window for an optimized seeding process, for enabling ultrathin UNCD.

In this context, a few reports were made very recently. Hees et al.[30] reported that the self-assembly of diamond nanoparticles onto the silicon dioxide surfaces was explained by a simple electrostatic attraction. Girard et al.[22] reported the electrostatic grafting of the nanodiamond particles (with the inherent negative charge on their surface) onto the substrate surface which was dip-coated with cationic polymer solution. Note that such electrostatic nature of the colloid particle, or that of the solid surface in contact with an electrolyte, is characterized using the concept of the *zeta potential*.[36,40,41] The present authors also have demonstrated that the nanodiamond dispersion on the Si substrate during ultrasonic treatment was strongly affected not only by the zeta potential of the seed particles but also by that of the pristine Si substrate surface.[42] By optimizing the dispersion by the choice of nanodiamond powder with a proper zeta potential, we have enabled an ultrathin (about 30 nm in thickness), void-free, and smooth UNCD deposition on the pristine Si substrate, using the DC-PACVD process with a hydrogen-rich gas chemistry.[42] The features and advantages of the DC-PACVD process for diamond synthesis are described elsewhere.[42−45] We have also shown that Si substrate surface modification by the hydrocarbon plasma or hydrocarbon thermal atmosphere adversely affected the seed dispersion,[42] in contrast to the previous report.[29]

Such results imply a good possibility of enabling a similar *ultrathin* UNCD coating on the *SiO_2 substrate*, using the same deposition process: via an analogous seeding technique, with some additional enhancement in the electrostatic interaction between the nanodiamond particle and the substrate. Nevertheless, it is not yet reported to date. In the present study, we investigated the effect of the surface modification of the SiO_2-coated Si substrate on the dispersed nanodiamond seed density prior to UNCD deposition, using the substrate exposure to the hydrogen as well as to the hydrocarbon. We show for the first time a successful synthesis of the void-free, ultrathin (30 nm in thickness) UNCD film on the SiO_2-coated Si substrate, by the DC-PACVD with the hydrogen-rich chemistry.

2. EXPERIMENTAL METHODS

The Si wafer [Grade: Prime, Diameter: 4 in., P-type/Boron dopant, Orientation: (100), Thickness: 0.5 mm, Resistivity: 1−10 Ω cm], SiO_2-coated Si wafer, and quartz wafer (i-Nexus, Inc., hydrothermal method, 2 in. in diameter, 0.5 mm in thickness, and double-side polished) were used as substrates. The SiO_2 layer formation on the Si wafer was carried out by using the sulfuric acid peroxide mixture (SPM) in wet station, to 20 nm in thickness. Prior to ultrasonic seeding, the substrates were exposed to the hydrogen plasma and the hydrocarbon plasma in the DC-PACVD chamber and to the hydrocarbon atmosphere in the HF-CVD chamber. The details of such pretreatments were shown in Table 1.

Subsequently, the substrates were ultrasonically seeded in the methanol suspension of nanodiamond powder (of approximately 3 nm in averaged diameter) for 1 h, followed by ultrasonic cleaning in ethanol three consecutive times for 30 s, respectively. The seed powder suspension was made by mixing 50 mg of nanodiamond powder with 200 mL of methanol under ultrasonic vibration.

UNCD deposition was carried out on the substrates by the DC-PACVD system, using a hydrogen-rich precursor gas mixture (gas composition: 3% CH_4 in H_2, total gas flow rate: 150 sccm) at the chamber pressure of 80 Torr, for the deposition time of 10−240 min. The DC discharge voltage and current were 450 V and 25 A, respectively. The structure and the process detail of the DC-PACVD were given elsewhere.[42−45] The discharge was maintained without the positive

dx.doi.org/10.1021/jp2117328 | J. Phys. Chem. C 2012, 116, 9180−9188

Table 2. Zeta Potentials Measured for Flat Substrates before and after the Treatments and for the Nanodiamond Colloid Particles in the Mutual Contact

	zeta potentials [mV] measured using monitor solution (latex particle + 10 mM NaCl aqueous solution)			zeta potentials [mV] measured using seeding suspension (nanodiamond particle + methanol)		
substrate	particle (ζ_P)	substrate (ζ_S)	$\zeta_P - \zeta_S$	particle (ζ_P)	substrate (ζ_S)	$\zeta_P - \zeta_S$
SiO_2/Si	−1.50	−28.30	+26.80	+30.01	−28.60	+58.61
*SiO_2/Si	−5.23	−31.03	+25.80	+37.51	−63.84	+101.35
†SiO_2/Si	+1.02	−22.71	+23.73	+1.82	−1.13	+2.95
‡SiO_2/Si	+4.26	−21.63	+25.89	+10.37	+14.85	−4.48

column at a short interelectrode distance of 5 mm.[44] The substrate temperature and cathode temperature were 780 ± 20 °C and 800 ± 20 °C, as measured at the lateral surfaces of the substrate holder and the cathode disk, respectively, by an optical pyrometer (MINOLTA TR-630A).

The zeta potentials of the nanodiamond suspension as well as that of the SiO_2-coated Si substrate surface before and after the pretreatments were measured by electrophoretic light scattering spectroscopy using the zeta potential analyzer (ELS-Z, Otsuka Electronics). The zeta potential analyzer was equipped with a quartz cell; its bottom could accommodate the substrate of which the zeta potential was to be measured (see the reference for the detail of the measuring technique).[46] The samples were cut into the size of 15 mm × 35 mm for the measurement. The nanodiamond−methanol suspension, which was used for the actual seeding in the present study, was used as a reference fluid (see Table 2). In addition, the 10 mM NaCl aqueous solution, dispersed with polystyrene latex reference particles of 520 nm in average diameter, was used as a standard monitor solution, for comparison. The pH of the diamond−methanol suspension was measured to be 7.5−8. Therefore, the pH of the standard monitor solution in comparison was also adjusted to the same level by adding 0.1 M NaOH. Smoluchowski's equation and Huckel's equation were used to calculate the zeta potentials of the substrates in contact with the standard monitor solution and that in contact with the nanodiamond−methanol suspension, respectively.

High-Resolution Scanning Electron Microscopy (HR-SEM, FEI Nova 200 NanoSEM), Near Edge X-ray Absorption Fine Structure Spectroscopy (NEXAFS, resolution: 0.1 eV, total electron yield mode, at the 7B1 KIST beamline of the Pohang Accelerator Laboratory in Republic of Korea), X-ray Photoelectron Spectroscopy (XPS, VG Multilab ESCA 2000 system using an Al Kα X-ray source), Fourier Transform Infrared Spectroscopy (FTIR, PerkinElmer, Spectrum 100 FTIR spectrometer), Raman Spectroscopy (Jobin Yvon T64000, wavelength of laser: 514.5 nm), High-Resolution Transmission Electron Microscopy (HR-TEM, TECNAI G2 F20, FEI, operated at 200 kV), and Energy Dispersive X-ray Spectroscopy (EDX, FEI) were employed to characterize the substrate surface before and after the treatments/seeding, as well as the coated UNCD film. The dispersed seed density on the substrate after the seeding was measured by image analysis software (Image Pro Plus) applied on the SEM images taken at five different spots on the sample substrate under the magnification of 50 000.

3. RESULTS AND DISCUSSION

Figure 1 compares the SEM microstructure of the UNCD layers coated on (a) the SiO_2-coated Si substrate against that coated on (b) the pristine Si substrates, both of which were not pretreated (see Table 1), although they were ultrasonically seeded prior to the deposition. In contrast to the well-developed continuous UNCD film formed on the Si substrate (Figure 1b), the large individual islands formed on the SiO_2 surface (Figure 1a) indicated a much lower initial nucleation density,[47] which was attributed to the lower dispersed seed density on the SiO_2 surface. It was obvious that a further improvement in the seeding technique was inevitable to achieve a well-developed continuous UNCD film on the SiO_2 surface. Increasing neither the ultrasonic seeding time nor the manual rinsing (instead of the ultrasonic cleaning subsequent to ultrasonic seeding, to reduce the loss of the seeds from the substrate) improved the poor nucleation on the SiO_2 surface.

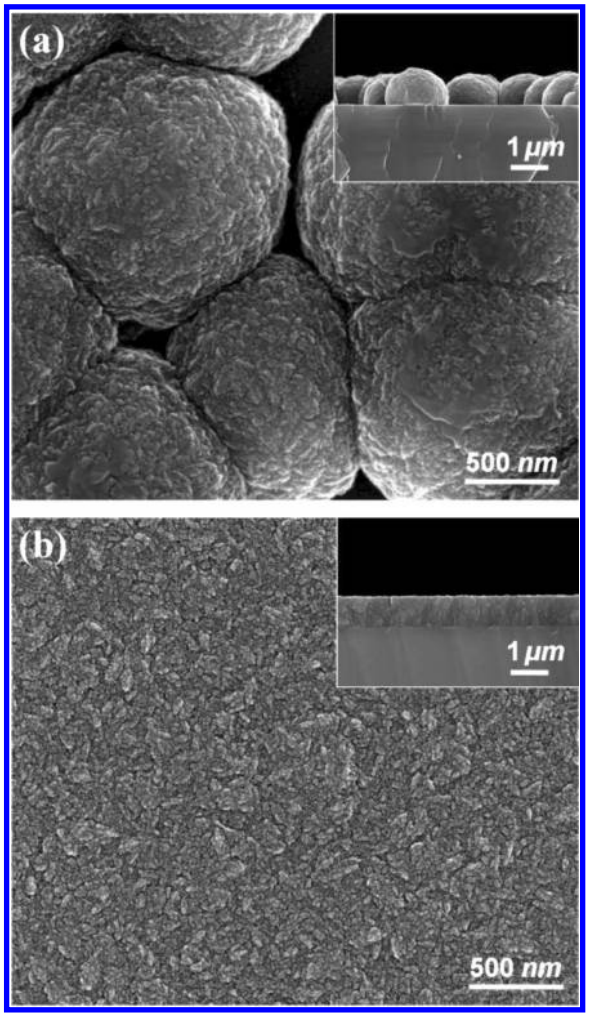

Figure 1. SEM images of the UNCD films synthesized for 4 h by DC-PACVD on (a) the SiO_2/Si substrate and (b) the pristine Si substrate.

Figure 2 shows the HR-SEM images of the dispersed nanodiamond particles on the SiO_2-coated Si substrates before

dx.doi.org/10.1021/jp2117328 | J. Phys. Chem. C 2012, 116, 9180−9188

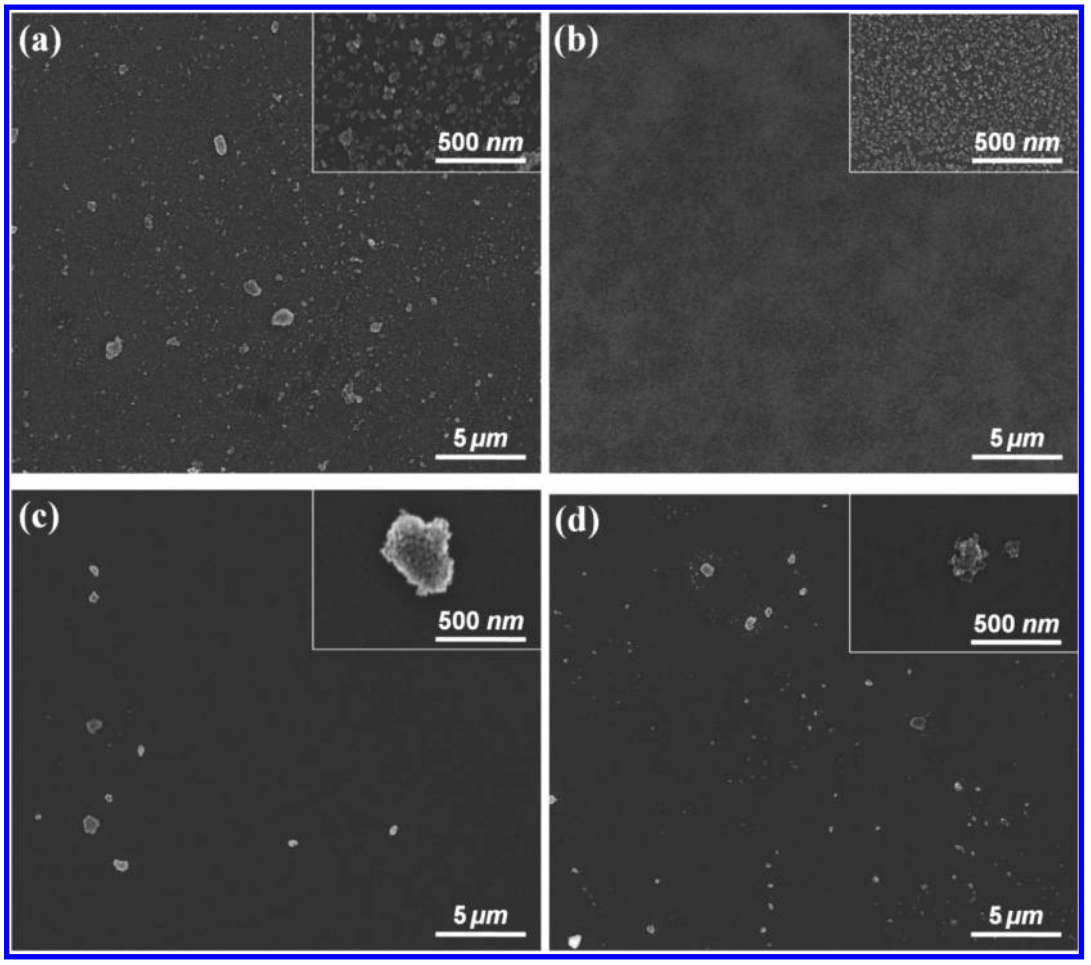

Figure 2. Dispersion of nanodiamond seed particles by ultrasonic treatment on the respective substrates [(a) pristine SiO_2/Si, (b) hydrogen-plasma-treated SiO_2/Si (*SiO_2/Si), (c) hydrocarbon-plasma-treated SiO_2/Si ($^{\dagger}SiO_2$/Si), and (d) hydrocarbon-thermal-treated SiO_2/Si ($^{\ddagger}SiO_2$/Si)].

and after the pretreatments: (a) untreated (denoted as SiO_2/Si); (b) treated by the hydrogen plasma (denoted as *SiO_2/Si); (c) treated by the hydrocarbon plasma (denoted as $^{\dagger}SiO_2$/Si); (d) thermally treated in hydrocarbon atmosphere (denoted as $^{\ddagger}SiO_2$/Si). The insets show the magnified view of the respective samples. It was remarkable that the dispersed seed densities varied drastically according to the respective surface pretreatments. The dispersed seed densities obtained from the images were (a) 7.8×10^{10}, (b) 4.8×10^{11}, (c) 3.2×10^{7}, and (d) 7.6×10^{8} nuclei/cm^2, respectively. The best result was obtained for the *SiO_2/Si (hydrogen plasma treatment), as shown in Figure 2b. The dispersed seed density on the *SiO_2/Si (Figure 2b) increased by a factor of 6 relative to that on the SiO_2/Si (Figure 2a). To the contrary, the seed densities on the substrate exposed to other pretreatments (Figure 2c and Figure 2d) were drastically reduced compared to that on the untreated substrate (Figure 2a). It was remarkable that not only the seed *densities* but also the seed *dispersion* (consequently the agglomeration) was sensitive to the treatments of the substrates.

Figure 3 compares HR-SEM images of the seeded SiO_2/Si (Figure 2a) and *SiO_2/Si (Figure 2b), after UNCD coating for 30 min by DC-PACVD, respectively. Note the pronounced effect of the hydrogen plasma treatment on the UNCD layer development, which might again be attributed to the seed dispersion densities on the respective substrates. Furthermore, when the SiO_2/Si and the *SiO_2/Si substrates, with *no* ultrasonic seeding, were subjected to the same deposition condition shown in Table 1, even as long as for 2 h, the diamond formations were negligible on both substrates. This indicated that the nucleation on some intrinsic nucleation center on the substrate, other than on the dispersed nanodiamond seeds, was negligible.

Figure 4a shows the plan-view HR-TEM image of the UNCD film shown in Figure 3b. The majority of the grains was less than 10 nm in diameter. The interplanar spacing shown in the inset was 2.06 Å, which corresponded to that of the diamond (111) planes. Figure 4b shows the NEXAFS C−K edge spectra taken from the same sample. The spectra taken from the HOPG (highly oriented pyrolytic graphite) were also shown for comparison. A sharp peak at 289.3 eV (C 1s → σ* transition) and the large dip at 302.2 eV (second absolute band gap) are the well-known fingerprints of diamonds.[48,49] A sharp peak at 285.5 eV (C 1s → π* transition) is observed for HOPG, whereas it is absent in the spectra taken from the UNCD sample.

One might as well attribute the drastic effect of the hydrogen plasma treatment to a complete removal of the surface SiO_2 layer by a possibly excessive plasma etching, with consequent exposure of the underlying Si. Indeed, one could not rule out such a possibility since the results shown in Figure 1 implied that the initial dispersed seed density, and the consequent nucleation on the pristine Si, was much more pronounced relative to that on the SiO_2 layer.

dx.doi.org/10.1021/jp2117328 | J. Phys. Chem. C 2012, 116, 9180−9188

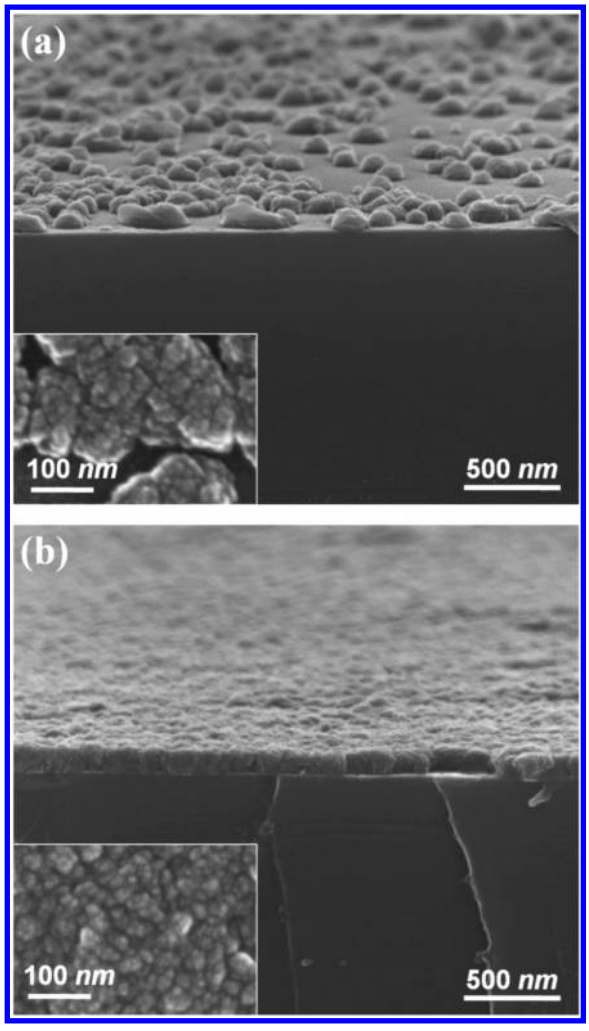

Figure 3. SEM images of the UNCD films synthesized for 30 min by DC-PACVD on the respective seeded substrates shown in Figure 2 [(a) pristine SiO_2/Si and (b) hydrogen-plasma-treated SiO_2/Si (*SiO_2/Si)].

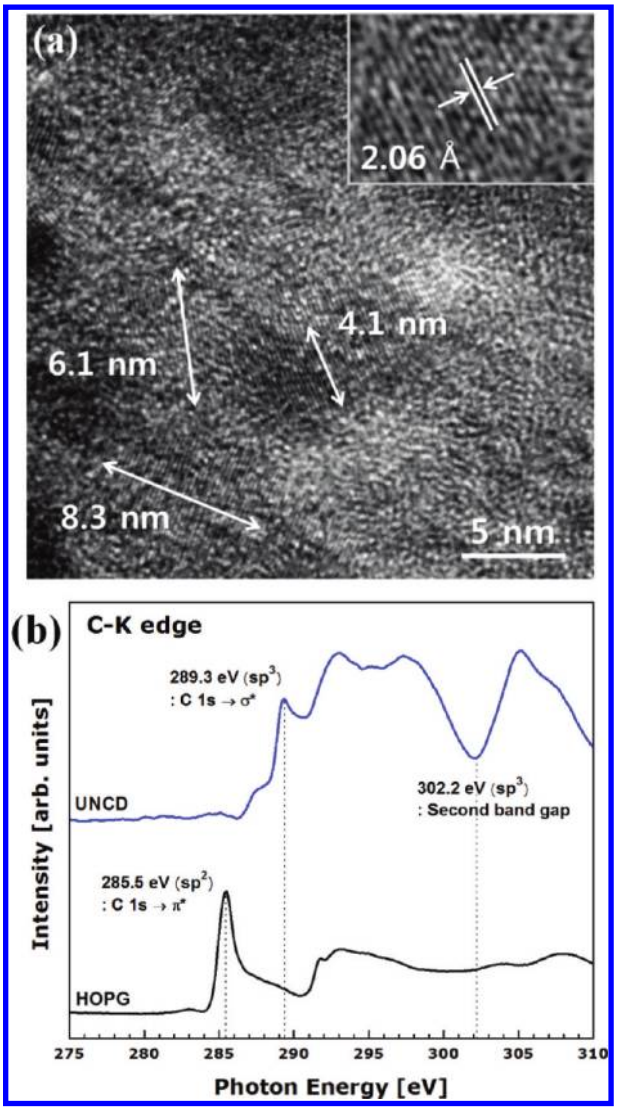

Figure 4. (a) HR-TEM plan-view image and (b) NEXAFS C−K edge spectra of the UNCD film shown in Figure 3b and HOPG.

However, such a possibility was ruled out by the cross-sectional TEM analysis (see Figure 5a) for the UNCD coated sample shown in Figure 3b. Four distinct layers were observed in the TEM image. Figure 5b shows the EDX profile taken along the solid arrow in Figure 5a. The oxygen profile was the highest in the layer II-2; its 20 nm thickness coincided with that of the original SiO_2 layer (see Section 2). It strongly suggested that it was a SiO_2 layer. Figure 5c shows the electron diffraction pattern taken from the area shown in Figure 5a, which was composed of the single crystalline Si diffraction spots, in addition to the continuous diffraction rings from the polycrystalline UNCD film. The EDX profile and the electron diffraction patterns indicated that the four layers in Figure 5a were (I) UNCD, (II-1) interlayer, (II-2) SiO_2, and (III) Si. The thickness of the SiO_2 layer after the treatment was largely the same as the one before the treatment (see Section 2), which confirmed that the seeding enhancement was not due to the total removal of the SiO_2 layer. On the other hand, it should be noted that a new dark layer of 2−3 nm in thickness was formed between the UNCD and the SiO_2 layer, which was denoted as the II-1 layer in Figure 5a. The exact nature of this layer should be studied further in the future.

Thus, the drastic enhancement of the dispersed seed density should be attributed to some modification of the molecular structure of the respective substrate surfaces, which will be described below. Figure 6a shows the XPS O 1s spectra taken on the surfaces of the pristine SiO_2/Si and *SiO_2/Si substrates prior to the seeding/UNCD deposition. Note that the peak in the spectrum of the nontreated SiO_2/Si substrate was symmetrical about 533.5 eV, which was typical of the Si−O bonding. By contrast, that from the *SiO_2/Si substrate was asymmetrical, with a contribution from an additional band, as shown in the inset. The new band around 531.5 eV indicated in the inset was attributed to the Si−OH group (also known as the silanol group[50]).[51,52] It was further supported by Figure 6b, which showed the NEXAFS O K-edge spectra taken from the same substrates. The small peak around 532 eV in the spectrum of *SiO_2/Si was also attributed to the silanol group.[51]

It was still further confirmed by the FTIR absorption spectra taken from the *SiO_2/Si substrate, as shown in Figure 7a. The spectrum from the pristine SiO_2/Si was subtracted from it as the background. The three dips at 974 cm^{-1} (Si−OH), 2260 cm^{-1} (SiO_3−H), and 3650 cm^{-1} (Si−OH) were attributed to the newly formed bonds on the *SiO_2/Si substrate relative to

dx.doi.org/10.1021/jp2117328 | J. Phys. Chem. C 2012, 116, 9180−9188

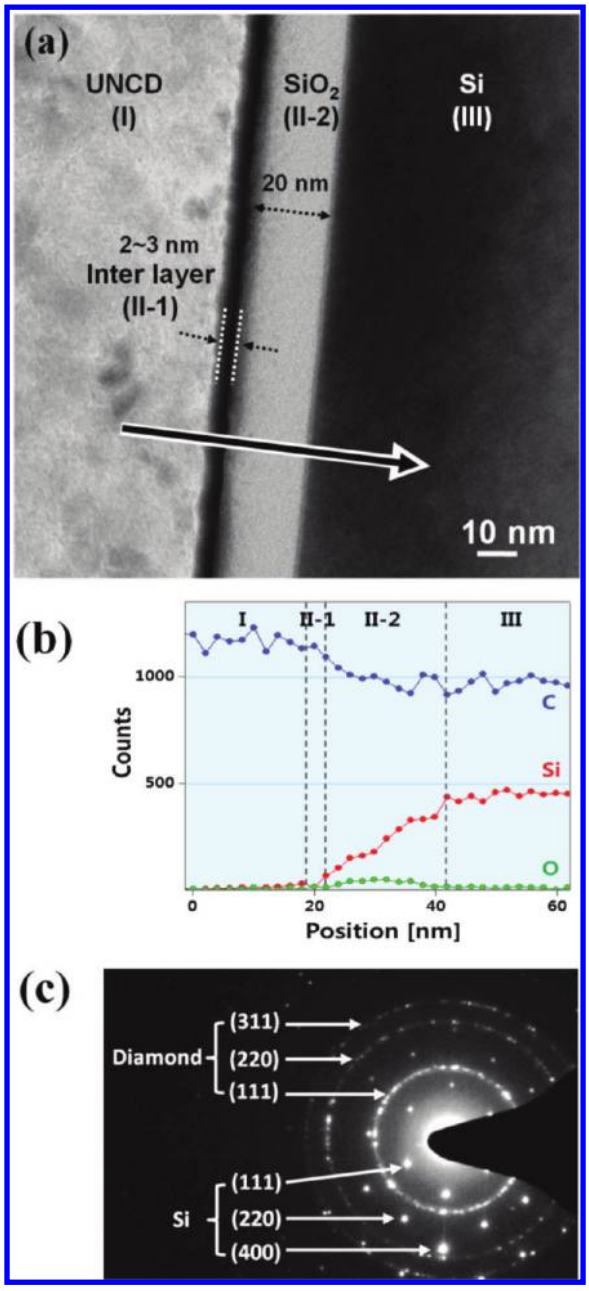

Figure 5. (a) HR-TEM cross-sectional image, (b) EDX spectroscopy, and (c) SAED pattern of the UNCD film shown in Figure 3b.

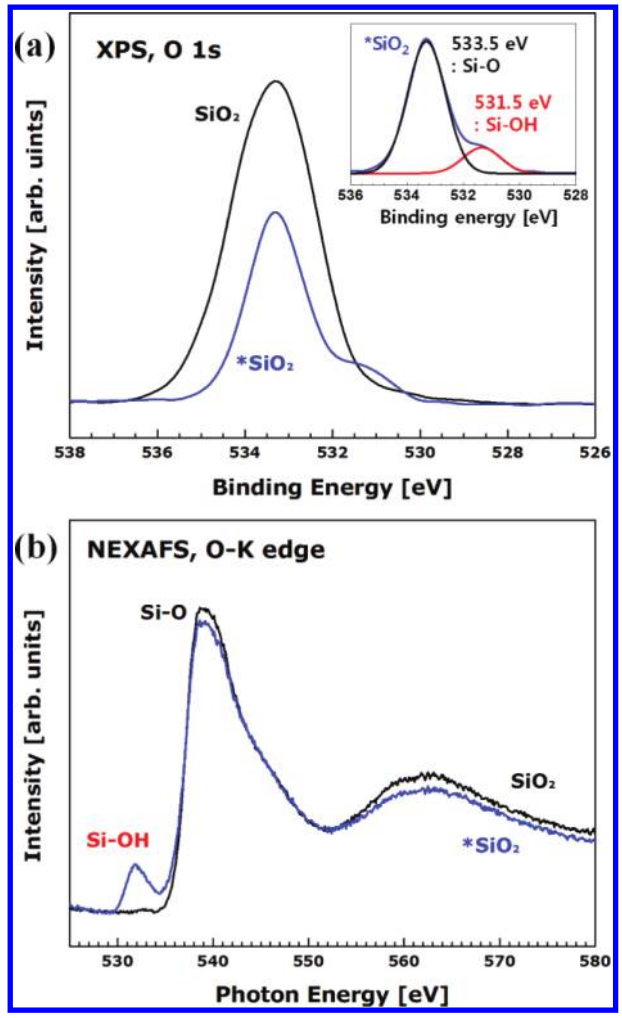

Figure 6. (a) XPS O 1s spectra and (b) NEXAFS O−K edge spectra of pristine SiO_2/Si and hydrogen-plasma-treated SiO_2/Si (*SiO_2/Si) substrates.

the pristine SiO_2/Si substrate, while the peak at 1050 cm^{-1} (Si−O−Si) was attributed to the *dip* present in the spectrum of the pristine SiO_2/Si substrate, which was subtracted as background.[53]

By contrast, the FTIR absorption spectra taken from the $^{\dagger}SiO_2$/Si and the $^{\ddagger}SiO_2$/Si substrate (see Figure 7b), where the spectrum from the pristine SiO_2/Si was also subtracted from it as the background, greatly differed from that shown in Figure 7a. The dips were observed at 775 and 1274 cm^{-1}, which were attributed to the Si−C and the C−H bond in $Si-CH_3$, respectively.[54,55] This indicated the carburization, as well as the $Si-CH_3$ termination on the surface of the substrates treated by the hydrocarbon plasma as well as that treated by the hydrocarbon thermal atmosphere.

Thus, it is evident that the hydrogen plasma treatment resulted in Si−OH termination, while the hydrocarbon plasma/thermal treatment resulted in the $Si-CH_3$ termination on the SiO_2 surfaces. One could easily expect that such new surface terminations would result in some modifications in the electrostatic nature of the surface, due to some difference in the polarities of the respective surface terminating groups. In the present study, the zeta potentials of such substrates were analyzed in two different ways, as shown in Table 2. The zeta potentials of the substrate surface (ζ_s), obtained by using the standard monitor solution as well as that measured by using the actual seeding suspension, were shown in Table 2. The former changed little, while the latter changed drastically, according to the respective surface pretreatments of the substrates. The former stayed within the relatively narrow range between −21.63 and −31.03 mV, while the latter widely varied from −63.84 to +14.85 mV.

It was also remarkable that the zeta potentials of the nanodiamond *particles* (ζ_p), measured by using the actual seeding suspension in contact with the respective substrates (see Section 2), were also strongly dependent on the respective *substrate surface* pretreatments: they widely varied from +1.82 to +37.51 mV. It indicated that the diamond particle and the substrate surface, both in contact with the liquid media of methanol, were mutually interacting electrostatically during the measurements, as well as in the actual ultrasonic seeding

dx.doi.org/10.1021/jp2117328 | J. Phys. Chem. C 2012, 116, 9180−9188

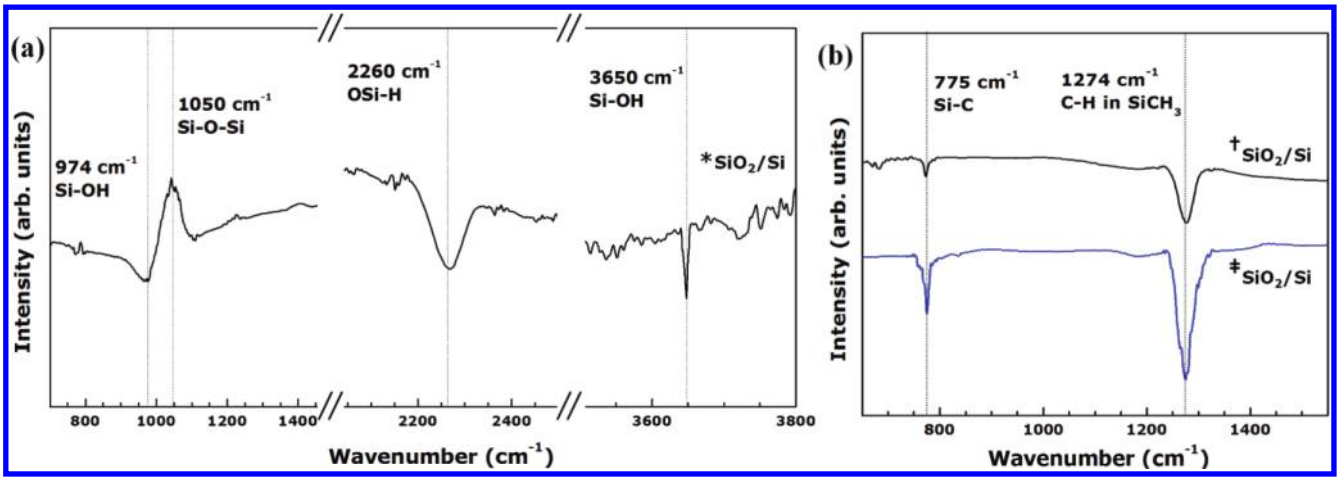

Figure 7. FTIR spectra of the (a) hydrogen-plasma-treated SiO_2/Si (*SiO_2/Si) substrate and (b) hydrocarbon-plasma-treated SiO_2/Si (†SiO_2/Si) and hydrocarbon-thermal-treated SiO_2/Si (‡SiO_2/Si) (signals from pristine SiO_2/Si substrate were subtracted as background).

process. Also note that the polarity of the zeta potential of the nanodiamond particle in the seeding suspension was positive, while those of the substrates in contact with the suspension were mostly negative, except for the ‡SiO_2/Si. The origin of such opposing polarity of the nanodiamond particle, with respect to that of the substrate, might be attributed to some surface state of, or some functional group present on, the particle surface, which is unknown presently.

Note that the zeta potential differences between the two ($\zeta_p - \zeta_s$), for the respective surface pretreatments, were the greatest for the hydrogen-plasma-treated substrate (+101.35 mV), sequentially followed by the pristine substrate (+58.61 mV) and the substrates pretreated by the hydrocarbon (+2.95 and −4.48 mV). Such a tendency exactly coincided with the order of the actual dispersed seed densities on the respective substrates, as described in relation to Figure 2 in the preceding paragraphs. It indicated that the dispersed seed density was dominated by the electrostatic interactions, as manifested in the zeta potential differences ($\zeta_p - \zeta_s$). The results agreed well with the previous report by Hees et al.,[30] who also showed a strong correlation between nucleation density and zeta potentials.

Note the drastically *increased* strength of the negative zeta potential of the *SiO_2/Si, relative to that of the SiO_2/Si. Clearly it should be attributed to the polarity of the Si−OH termination on the *SiO_2 surface. It was reported that the surface silanol groups on the fused silica surface undergo protolysis, so that the OH^- ions adsorb on the surface (see the Introduction section of the reference).[56] Schwer et al.[57] reported that the zeta potential of the fused silica substrate was negative in the aqueous as well as in the methanol−water solution, for a wide range of pH of 3−11; for a 50% methanol−water solution, the zeta potential of the fused silica was around −60 mV at the pH of 8 (see Figure 10 of the reference). Although they did not mention the Si−OH termination on their fused silica surface, Parks[58] pointed out that the anhydrous oxides of metal can become hydrated in several ways to form an M−OH termination (M: metal) on its surface, which might as well occur during exposure to aqueous solution (see Section II-B-2 of the reference). It indicated that the fused silica surface in Schwer et al.'s report[57] might have also contained Si−OH terminations. It follows that the enhanced strength of the negative zeta potential of the Si−OH terminated *SiO_2/Si in the present study might be attributed to the negative polarity of the newly formed Si−OH termination.

By contrast, note the drastically *decreased* strengths of the negative zeta potential of †SiO_2/Si. Furthermore, the polarity of zeta potential of ‡SiO_2/Si was even reversed (see Table 2). It strongly suggested that the polarity of the Si−CH_3 termination, induced by the exposure to the hydrocarbon plasma or by the hydrocarbon thermal atmosphere (aforementioned in relation to Figure 7b), was opposite to that of the Si−OH termination. Indeed, Hozumi et al.[46] reported that the Si−CH_3 termination on the SiO_2-coated Si substrate surface shifted its *negative* zeta potential toward the *positive* direction by no less than around +20 mV (see Figure 2 of the reference) for the wide pH range of 3−11 (recall that the pH of the seeding solution in the present study was 7.5−8). It indicated that the polarity of the Si−CH_3 termination in the present study was positive. It follows that the decreasing strength of negative zeta potential of †SiO_2/Si, or the even reversed polarity of the zeta potential of ‡SiO_2/Si in the present study, should be attributed to such positive polarity of the Si−CH_3 termination, as opposed to that of the Si−OH termination.

On the other hand, it is well-known that the zeta potential is sensitive to the pH of the monitor solution,[46,57,59,60] which might be, in turn, altered by the dispersion of the colloid particles with certain zeta potential. Indeed, Chakrapani et al.[61] reported that the dispersion of the hydrogen-terminated diamond powder in the solution increased its pH from 5 to 8.5; it also affected the measured zeta potential of the colloid particles. It indicated the possibility that Si−OH or Si−CH_3 termination of the substrate surface might have altered the pH of the seeding suspension. However, the pHs of the seeding suspensions, both before and after the contact with the respective substrates, fell in the range of 7.5−8 in the present study; it ruled out the possibility.

Note that the magnitude of the positive zeta potentials of the *nanodiamond particle* in the seeding suspension were significantly increased for SiO_2/Si and *SiO_2/Si, relative to those for †SiO_2/Si or ‡SiO_2/Si (see Table 2). The origin of such behavior is not clear presently, although it is obviously attributed to some electrostatic interaction between the two. Nevertheless, it is in good agreement with the enhanced *dispersion* of the seeds on the SiO_2/Si and *SiO_2/Si, apart from their enhanced seed dispersion *density*, as indicated in the

dx.doi.org/10.1021/jp2117328 | J. Phys. Chem. C 2012, 116, 9180−9188

preceding paragraphs in relation to the microstructures shown in the insets of Figure 2. It is not surprising since electrostatic repulsion between the individual colloid particles, and hence their dispersion, would increase with the zeta potential.

Figure 8 shows the ultrathin UNCD film synthesized on the quartz substrate pretreated by the hydrogen plasma prior to the seeding, as indicated in Section 2. The film was synthesized under the same deposition condition shown in Table 2, for the deposition time as short as 10 min. The film was smooth, void-free, and well adherent. The thickness of the film was less than 30 nm as evident from Figure 8a, which was the thinnest among the void-free UNCD films coated on the SiO_2 substrate reported to date. Figure 8b shows the Raman spectra (λ = 514.5 nm) taken from the sample. Apart from the usual D and G bands, extra peaks at 1138, 1332, and 1482 cm^{-1} were observed which were typical in UNCD with grain size below 10 nm.[45,62−64]

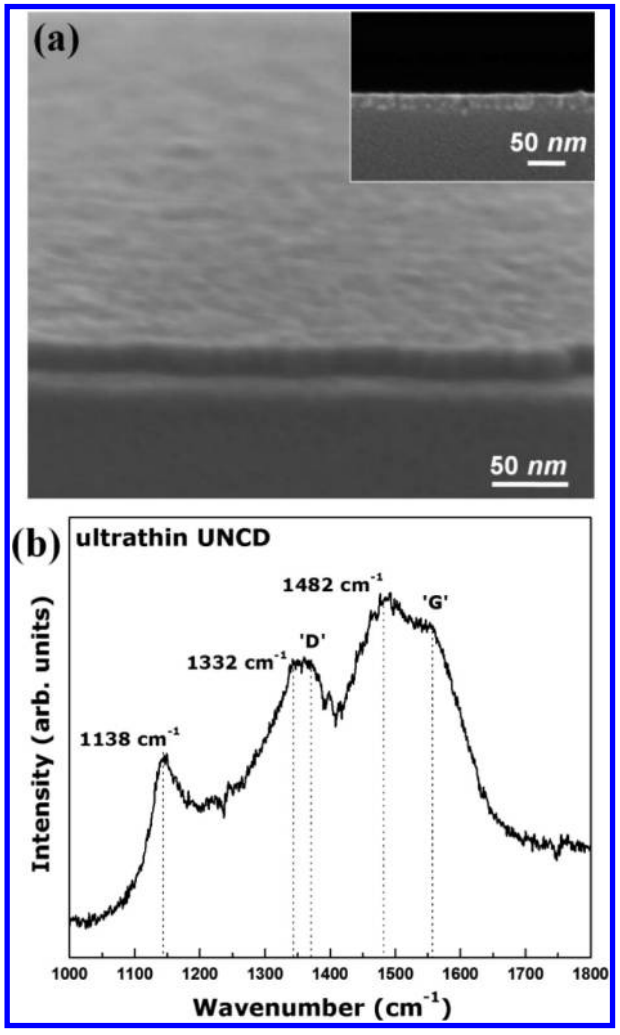

Figure 8. (a) HR-SEM images and (b) Raman spectra of the ultrathin (about 30 nm in thickness) UNCD film on the quartz substrate pretreated by hydrogen plasma using DC-PACVD prior to the ultrasonic treatment and subsequent UNCD deposition for 10 min by DC-PACVD.

4. CONCLUSIONS

The exposure of the SiO_2-coated Si wafer to the hydrogen plasma, prior to the ultrasonic seeding, drastically enhanced the density of the dispersed nanodiamond seeds on its surface. Such drastic enhancement in the seeding density was attributed to the modification of the zeta potentials of the substrate surfaces due to the formation of the silanol group on the SiO_2 surface. It not only increased the strength of the negative zeta potential of the *substrate* but also favorably altered that of the nanodiamond particle in the suspension, in contact with the substrate. It consequently enhanced the electrostatic attraction of the nanodiamond particle to the substrate, as well as their electrostatic dispersion on the surface. It eventually enabled the void-free ultrathin UNCD coating as thin as 30 nm on the SiO_2-coated Si wafer by DC-PACVD using hydrogen-rich gas chemistry.

AUTHOR INFORMATION

Corresponding Author

*Tel.: +82-2-958-5497. Fax: +82-2-958-5509. E-mail: wsleemk@gmail.com.

Notes

The authors declare no competing financial interest.

ACKNOWLEDGMENTS

This work was supported by a grant (code No.: 2011K000174) from the 'Center for Nanostructured Materials and Technology' under '21st Century Frontier R&D Programs' of the Ministry of Education, Science and Technology, Korea. This work was also supported by an institutional program grant (2E22733) from the Korea Institute of Science and Technology.

REFERENCES

(1) Gruen, D. M. *Annu. Rev. Mater. Sci.* **1999**, *29*, 211.
(2) Gruen, D. M. *MRS Bull.* **1998**, *23*, 32.
(3) Auciello, O.; Sumant, A. V. *Diamond Relat. Mater.* **2010**, *19*, 699.
(4) Williams, O. A.; Nesladek, M. *Phys. Status Solidi A* **2006**, *203*, 3375.
(5) Butler, J. E.; Sumant, A. V. *Chem. Vap. Deposition* **2008**, *14*, 145.
(6) Railkar, T. A.; Kang, W. P.; Windischmann, H.; Malshe, A. P.; Naseem, H. A.; Davidson, J. L.; Brown, W. D. *Crit. Rev. Solid State Mater. Sci.* **2000**, *25*, 163.
(7) Sekaric, L.; Parpia, J. M.; Craighead, H. G.; Feygelson, T.; Houston, B. H.; Butler, J. E. *Appl. Phys. Lett.* **2002**, *81*, 4455.
(8) Sumant, A. V.; Auciello, O.; Carpick, R. W.; Srinivasan, S.; Butler, J. E. *MRS Bull.* **2010**, *35*, 281.
(9) Kromka, A.; Rezek, B.; Remes, Z.; Michalka, M.; Ledinsky, M.; Zemek, J.; Potmesil, J.; Vanecek, M. *Chem. Vap. Deposition* **2008**, *14*, 181.
(10) Philip, J.; Hess, P.; Feygelson, T.; Butler, J. E.; Chattopadhyay, S.; Chen, K. H.; Chen, L. C. *J. Appl. Phys.* **2003**, *93*, 2164.
(11) Zhou, D. D.; Greenberg, R. J. *Front. Biosci.* **2005**, *10*, 166.
(12) Bergonzo, P.; Bongrain, A.; Scorsone, E.; Bendali, A.; Rousseau, L.; Lissorgues, G.; Mailley, P.; Li, Y.; Kauffmann, T.; Goy, F.; et al. *Irbm* **2011**, *32*, 91.
(13) Ganesan, K.; Stacey, A.; Meffin, H.; Lichter, S.; Greferath, U.; Fletcher, E. L.; Prawer, S. *IEEE Eng. Med. Biol.* **2010**, 6757.
(14) Szunerits, S.; Ghodbane, S.; Niedziolka-Jonsson, J.; Galopin, E.; Klauser, F.; Akjouj, A.; Pennec, Y.; Djafari-Rouhani, B.; Boukherroub, R.; Steinmuller-Nethl, D. *J. Phys. Chem. C* **2010**, *114*, 3346.
(15) Ternyak, O.; Akhvlediani, R.; Hoffman, A. *Diamond Relat. Mater.* **2005**, *14*, 323.
(16) Catledge, S. A.; Vohra, Y. K.; Mirkarimi, P. B. *J. Phys. D: Appl. Phys.* **2005**, *38*, 1410.
(17) Lee, J. S.; Liu, K. S.; Lin, I. N. *J. Appl. Phys.* **1997**, *81*, 486.
(18) Stoner, B. R.; Ma, G. H. M.; Wolter, S. D.; Glass, J. T. *Phys. Rev. B* **1992**, *45*, 11067.

(19) Bongrain, A.; Scorsone, E.; Rousseau, L.; Lissorgues, G.; Gesset, C.; Saada, S.; Bergonzo, P. *J. Micromech. Microeng.* **2009**, *19*.
(20) Liu, Y. K.; Tso, P. L.; Lin, I. N.; Tzeng, Y.; Chen, Y. C. *Diamond Relat. Mater.* **2006**, *15*, 234.
(21) Chen, Y. C.; Zhong, X. Y.; Konicek, A. R.; Grierson, D. S.; Tai, N. H.; Lin, I. N.; Kabius, B.; Hiller, J. M.; Sumant, A. V.; Carpick, R. W.; Auciello, O. *Appl. Phys. Lett.* **2008**, *92*, 133113.
(22) Girard, H. A.; Perruchas, S.; Gesset, C.; Chaigneau, M.; Vieille, L.; Arnault, J. C.; Bergonzo, P.; Boilot, J. P.; Gacoin, T. *ACS Appl. Mater. Interfaces* **2009**, *1*, 2738.
(23) Srivastava, J. K.; Prasad, M.; Wagner, J. B. *J. Electrochem. Soc.* **1985**, *132*, 955.
(24) Jiang, N.; Noguchi, S.; Nishimura, K.; Inaoka, T.; Shintani, Y.; Hiraki, A. *Jpn. J. Appl. Phys. 1* **2002**, *41*, 6493.
(25) Yugo, S.; K., T.; Kanai, H. *Sci. Technol. New Diamond* **1990**, 119.
(26) Iijima, S.; Aikawa, Y.; Baba, K. *Appl. Phys. Lett.* **1990**, *57*, 2646.
(27) Williams, O. A.; Douheret, O.; Daenen, M.; Haenen, K.; Osawa, E.; Takahashi, M. *Chem. Phys. Lett.* **2007**, *445*, 255.
(28) Krueger, A. *J. Mater. Chem.* **2008**, *18*, 1485.
(29) Sumant, A. V.; Gilbert, P.; Grierson, D. S.; Konicek, A. R.; Abrecht, M.; Butler, J. E.; Feygelson, T.; Rotter, S. S.; Carpick, R. W. *Diamond Relat. Mater.* **2007**, *16*, 718.
(30) Hees, J.; Kriele, A.; Williams, O. A. *Chem. Phys. Lett.* **2011**, *509*, 12.
(31) Greiner, N. R.; Phillips, D. S.; Johnson, J. D.; Volk, F. *Nature* **1988**, *333*, 440.
(32) Kuznetsov, V. L.; Aleksandrov, M. N.; Zagoruiko, I. V.; Chuvilin, A. L.; Moroz, E. M.; Kolomichuk, V. N.; Likholobov, V. A.; Brylyakov, P. M.; Sakovitch, G. V. *Carbon* **1991**, *29*, 665.
(33) Shenderova, O.; Hens, S.; McGuire, G. *Diamond Relat. Mater.* **2010**, *19*, 260.
(34) Avdeev, M. V.; Rozhkova, N. N.; Aksenov, V. L.; Garamus, V. M.; Willumeit, R.; Osawa, E. *J. Phys. Chem. C* **2009**, *113*, 9473.
(35) Ozawa, M.; Inaguma, M.; Takahashi, M.; Kataoka, F.; Krüger, A.; Ōsawa, E. *Adv. Mater.* **2007**, *19*, 1201.
(36) Neugart, F.; Zappe, A.; Jelezko, F.; Tietz, C.; Boudou, J. P.; Krueger, A.; Wrachtrup, J. *Nano Lett.* **2007**, *7*, 3588.
(37) Xu, Y. Y.; Yu, Z. M.; Zhu, Y. M.; Wang, B. C. *Diamond Relat. Mater.* **2005**, *14*, 206.
(38) Krüger, A.; Kataoka, F.; Ozawa, M.; Fujino, T.; Suzuki, Y.; Aleksenskii, A. E.; Vul, A. Y.; Osawa, E. *Carbon* **2005**, *43*, 1722.
(39) Williams, O. A.; Hees, J.; Dieker, C.; Jager, W.; Kirste, L.; Nebel, C. E. *ACS Nano* **2010**, *4*, 4824.
(40) McGown, D. N. L.; Parfitt, G. D.; Willis, E. *J. Colloid Sci.* **1965**, *20*, 650.
(41) Meadus, F. W.; Puddington, I. E.; Sirianni, A. F.; Sparks, B. D. *J. Colloid Interface Sci.* **1969**, *30*, 46.
(42) Lee, H.-J.; Jeon, H.; Lee, W.-S. *J. Appl. Phys.* **2011**, *110*, 084305.
(43) Lee, W. S.; Chae, K. W.; Baik, Y. J.; Park, J. K. *Diamond Relat. Mater.* **2010**, *19*, 1168.
(44) Lee, H.-J.; Jeon, H.; Lee, W.-S. *J. Appl. Phys.* **2011**, *109*, 023303.
(45) Lee, H.-J.; Li, H.; Jeon, H.; Lee, W.-S. *Diamond Relat. Mater.* **2010**, *19*, 1393.
(46) Hozumi, A.; Sugimura, H.; Yokogawa, Y.; Kameyama, T.; Takai, O. *Colloids Surf., A* **2001**, *182*, 257.
(47) Kulisch, W.; Popov, C. *Phys. Status Solidi A* **2006**, *203*, 203.
(48) Sumant, A. V.; Grierson, D. S.; Gerbi, J. E.; Birrell, J.; Lanke, U. D.; Auciello, O.; Carlisle, J. A.; Carpick, R. W. *Adv. Mater.* **2005**, *17*, 1039.
(49) Adiga, V. P.; Sumant, A. V.; Suresh, S.; Gudeman, C.; Auciello, O.; Carlisle, J. A.; Carpick, R. W. *Phys. Rev. B* **2009**, *79*, 245403.
(50) Boehm, H. P. *Angew. Chem., Int. Ed. Engl.* **1966**, *5*, 533.
(51) Carniato, S.; Gallet, J. J.; Rochet, F.; Dufour, G.; Bournel, F.; Rangan, S.; Verdini, A.; Floreano, L. *Phys. Rev. B* **2007**, *76*.
(52) Erdem, B.; Hunsicker, R. A.; Simmons, G. W.; Sudol, E. D.; Dimonie, V. L.; El-Aasser, M. S. *Langmuir* **2001**, *17*, 2664.
(53) Michalak, D. J.; Amy, S. R.; Esteve, A.; Chabal, Y. J. *J. Phys. Chem. C* **2008**, *112*, 11907.
(54) Chua, C. T.; Sarkar, G.; Chooi, S. Y. M.; Chan, L. *J. Mater. Sci. Lett.* **1999**, *18*, 33.
(55) Grill, A.; Neumayer, D. A. *J. Appl. Phys.* **2003**, *94*, 6697.
(56) Schutzner, W.; Kenndler, E. *Anal. Chem.* **1992**, *64*, 1991.
(57) Schwer, C.; Kenndler, E. *Anal. Chem.* **1991**, *63*, 1801.
(58) Parks, G. A. *Chem. Rev.* **1965**, *65*, 177.
(59) Elimelech, M.; Chen, W. H.; Waypa, J. J. *Desalination* **1994**, *95*, 269.
(60) Kirby, B. J.; Hasselbrink, E. F. *Electrophoresis* **2004**, *25*, 187.
(61) Chakrapani, V.; Angus, J. C.; Anderson, A. B.; Wolter, S. D.; Stoner, B. R.; Sumanasekera, G. U. *Science* **2007**, *318*, 1424.
(62) Zeng, L. Y.; Peng, H. Y.; Wang, W. B.; Chen, Y. Q.; Lei, D.; Qi, W. T.; Liang, J. Q.; Zhao, J. L.; Kong, X. G.; Zhang, H. *J. Phys. Chem. C* **2008**, *112*, 1401.
(63) May, P. W.; Ashfold, M. N. R.; Mankelevich, Y. A. *J. Appl. Phys.* **2007**, *101*, 053115.
(64) Michaelson, S.; Stacey, A.; Orwa, J.; Cimmino, A.; Prawer, S.; Cowie, B. C. C.; Williams, O. A.; Gruen, D. M.; Hoffman, A. *J. Appl. Phys.* **2010**, *107*.